Structure, Electrochemistry and Hydroformylation Catalytic Activity of the Bis(pyrazolylborato)rhodium(I) Complexes [RhBp(CO)P] [P = $P(NC_4H_4)_3$, PPh_3, PCy_3, $P(C_6H_4OMe\text{-}4)_3$]

Anna M. Trzeciak,*[a] Beata Borak,[a] Zbigniew Ciunik,[a] Józef J. Ziółkowski,[a] M. Fátima C. Guedes da Silva,[b,c] and Armando J. L. Pombeiro[b]

Keywords: Rhodium / N ligands / Electrochemistry / X-ray diffraction / Hydroformylation

Rhodium complexes of formula [RhBp(CO)P] [Bp = bis(pyrazolylborate), P = $P(NC_4H_4)_3$ **1**, PPh_3 **2**, PCy_3 **3**, $P(C_6H_4OMe\text{-}4)_3$ **4**] have been prepared by exchange of the acetylacetonate ($acac^-$) ligand in [Rh(acac)(CO)P] complexes. The spectroscopic and electrochemical properties as well as X-ray data of [Rh(acac)(CO)P] and [RhBp(CO)P] complexes have been compared with the aim to estimate the relative donor properties of both anionic ligands ($acac^-$ and Bp^-). The cyclic voltammetric results indicate that the Bp^- ligand behaves as a much stronger electron donor than $acac^-$ and a value of the Lever E_L ligand parameter identical to that of the pyrazolate ligand (–0.24 V vs. NHE for each coordinating arm) is proposed for the bis- and tris(pyrazolyl)borate ligands, whereas $P(C_6H_4OMe\text{-}4)_3$ is also shown to have an identical E_L value (0.69 V) to that of $P(NC_4H_4)_3$. An improved linear relationship between the oxidation potential and the sum of the ligand E_L values for square-planar Rh^I complexes is also obtained and adjusted values for the Lever S_M and I_M parameters for the Rh^I/Rh^{II} redox couple are given. The *trans* influence of phosphanes was not observed in crystals of complexes **2** and **3**, in contrast to analogous acetylacetonato complexes in which the Rh–O bonds differ by ca. 0.04–0.06 Å. Complexes **1**–**4** are very attractive precursors for hydroformylation catalysts and yields of aldehydes of 80–87% have been obtained with all complexes without extra phosphane as co-catalyst. During the hydroformylation reaction, however, small amounts of a catalytically inactive $[RhBp(CO)_2]$ complex were formed.

Introduction

The exceptionally high catalytic activity of rhodium complexes in the hydroformylation of unsaturated compounds is well known.[1] Among the large number of rhodium catalyst precursors, the acetylacetonato complexes $[Rh(acac)(CO)_2]$, [Rh(acac)(CO)P] or $[Rh(acac)P_2]$ (acac: acetylacetonato, P: phosphorus ligands) are used very often, both in the laboratory and in industrial processes.[2−4] Many studies have shown that the acetylacetonato ligand is easily removed from the coordination sphere of rhodium in the presence of CO and H_2, facilitating the formation of active hydrido-carbonyl complexes.[5,6] In contrast to rhodium complexes with anionic oxygen-containing ligands, there are very few data reporting the application of rhodium complexes containing nitrogen ligands as catalyst precursors. The few known examples, including the active rhodium pyrazolylborate complexes in the high pressure hydroformylation of propylene (60−80 atm of H_2/CO) and 1-hexene (30−50 atm of H_2/CO), have been patented.[7]

Tris(pyrazolylborato) ligands are very often compared with cyclopentadienyl ligands in view of their similar electronic structure and steric properties.[8,9]

In this paper we report the results of structural as well as catalytic studies of rhodium bis(pyrazolylborate) complexes of the type [RhBp(CO)P] [Figure 1; Bp: bis(pyrazolylborate), P: $P(NC_4H_4)_3$ **1**, PPh_3 **2**, PCy_3 **3**, $P(C_6H_4OMe\text{-}4)_3$ **4**].

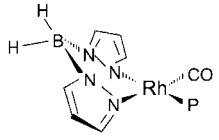

Figure 1. Structure of [RhBp(CO)P] complexes

We were also interested in comparing the properties of these complexes with those of a known family of square-

[a] Faculty of Chemistry, University of Wrocław,
14 F. Joliot-Curie St., 50-383 Wrocław, Poland
Fax: (internat.) + 48-71-375-7356
E-mail: jjz@wchuwr.chem.uni.wroc.pl
[b] Centro de Química Estrutural, Complexo I, Instituto Superior Técnico,
Av. Rovisco Pais, 1049-001 Lisboa, Portugal
E-mail: pombeiro@ist.utl.pt
[c] Universidade Lusófona de Humanidades e Tecnologias,
Av. Campo Grande 376, 1749-024 Lisboa, Portugal
E-mail: fatima.guedes@ist.utl.pt

planar rhodium complexes of formula [Rh(acac)(CO)P] (P: phosphorus ligand). In both types of complexes the rhodium(I) ion is coordinated by the chelating ligand through two nitrogen or oxygen atoms, forming a six-membered ring. Rhodium(I) complexes with β-diketonate ligands are known as model groups of rhodium complexes for which the *trans* effect, the effect of the steric and electronic properties of the phosphorus ligands, as well as the electrochemical, thermochemical and kinetic properties, have been discussed.[10−14] However, rhodium(I) complexes with bis(pyrazolylborato) ligands, although known for a long time, have not received any special attention.

Results and Discussion

Strategy of Synthesis

Complexes **1** and **4** were prepared and characterized for the first time in this paper (details in Exp. Sect.). Complex **2** was obtained earlier by reaction of $[RhCl(CO)_2]_2$ with KBp.[15,16] We adapted the other method of synthesis of [RhBp(CO)P] complexes, reported recently for $[RhTp^{Ph,Me}(CO)_2]$ and $[RhTp^{Ph,Me}(CO)(PPh_3)]$, based on the replacement of an $acac^-$ ligand by a bis(pyrazolylborate).[17] The reactions were performed with isolated [Rh(acac)(CO)P] complexes, at room temperature, and were complete in ca. 30 min, giving satisfactory yields of pure products.

Alternatively, the complexes [Rh(acac)(CO)P] were prepared "in situ" from $[Rh(acac)(CO)_2]$ and the appropriate amount of the phosphorus ligand P and further used for the substitution of anionic ligands ($acac^-$ for Bp^-; Scheme 1).

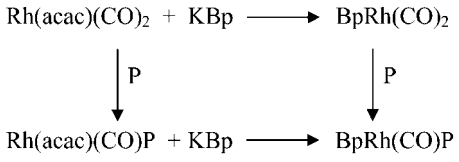

Scheme 1. Synthesis of [RhBp(CO)P] complexes

The third method of synthesis of the complexes consisted of the reaction of $[Rh(acac)(CO)_2]$ with KBp to give $[RhBp(CO)_2]$, followed by replacement of CO by the phosphane P. Independent of the reaction pathway, the [RhBp(CO)P] complexes were isolated as final products with yields of 70−90%.

IR and ^{31}P NMR Spectra

The ν(CO) frequencies in the IR spectra of [RhBp(CO)P] complexes are summarized in Table 1, where the IR data of analogous [Rh(acac)(CO)P] complexes are also presented for comparison. The ν(CO) frequencies in the bis(pyrazolylborato) complexes decrease with an increase of the σ/π-donor properties of the P ligands in the order $P(NC_4H_4)_3 > PPh_3 > P(C_6H_4OMe\text{-}4)_3 > PCy_3$. Similar changes of ν(CO) frequencies were observed in the IR spectra of [Rh(acac)(CO)P] and [Rh{$CF_3C(O)CHC(NH)Me$}(CO)P] complexes.[18] The highest ν(CO) frequencies were found for complexes with the Bp^- ligand, if rhodium compounds with the same phosphane ligand were compared. The positions of the IR bands suggest a weaker σ/π-donor character of the *N*,*N*-Bp^- ligand in comparison with *O*,*O*-$acac^-$ and *N*,*O*-bonded ones (β-ketoiminate). However, a more detailed analysis of the $J_{Rh,P}$ coupling constants in the ^{31}P NMR spectra leads to another conclusion. The $J_{Rh,P}$ coupling constants determined for [RhBp(CO)P] complexes are similar to those for β-ketoiminato complexes but lower than the corresponding $J_{Rh,P}$ values for acetylacetonato complexes (Table 1). Usually, $J_{Rh,P}$ decreases when the ligand σ/π-donor character increases. Therefore, according to this criterion, the *N*,*N*-Bp^- ligand should be a more effective donor than the *O*,*O*-acetylacetonato ligand, which is in agreement with the electrochemical results discussed below.

Following Tolman's rule for complexes in which the electronic effect dominates, the $J_{Rh,P}$ values decrease with a decrease of ν(CO) frequencies.[19] Such a dependence has been observed previously for both [Rh(acac)(CO)P] and [RhBp(CO)P] complexes (Figure 2). However, the plot of the experimental data fits not one curve but two almost parallel ones.

^1H NMR Spectra

The ^1H NMR spectra of complexes **1**−**4** contain six signals due to the inequivalent protons of the pyrazolyl rings. All resonances are located in the δ = 5.7−7.6 ppm range, similar to what was observed for other bis(pyrazolylborato) rhodium complexes (Table 2). The two signals of the 4-H protons are shifted upfield with respect to the remaining signals and are observed at ca. δ = 6 ppm. In all spectra

Table 1. IR and ^{31}P NMR spectroscopic data of [Rh(acac)(CO)P],[5,39] [RhBp(CO)P] and [Rh(N,O)(CO)P][18]

P	Rh(acac)(CO)P ν(CO) (cm^{-1})	Rh(acac)(CO)P δ (ppm) ($J_{Rh,P}$, Hz)	[RhBp(CO)P] ν(CO) (cm^{-1})	[RhBp(CO)P] δ (ppm) ($J_{Rh,P}$, Hz)	[Rh(N,O)(CO)P] (P *trans* to N) ν(CO) (cm^{-1})	[Rh(N,O)(CO)P] (P *trans* to N) δ (ppm) ($J_{Rh,P}$, Hz)	[Rh(N,O)(CO)P] (P *trans* to O) δ (ppm) ($J_{Rh,P}$, Hz)
$P(NC_4H_4)_3$	2008	102 (251.8)	2018	104 (224)	2001	104.3 (217.4)	107.5 (247.7)
PPh_3	1983	46 (177.4)	1987	44 (156)	1973	45.6 (150.7)	60.5 (175.3)
$P(C_6H_4\text{-}4\text{-}OMe)_3$	1964	41 (173)	1983	36 (154)			
PCy_3	1945	58 (170)	1966	51 (147)	1946	55.8 (143.7)	

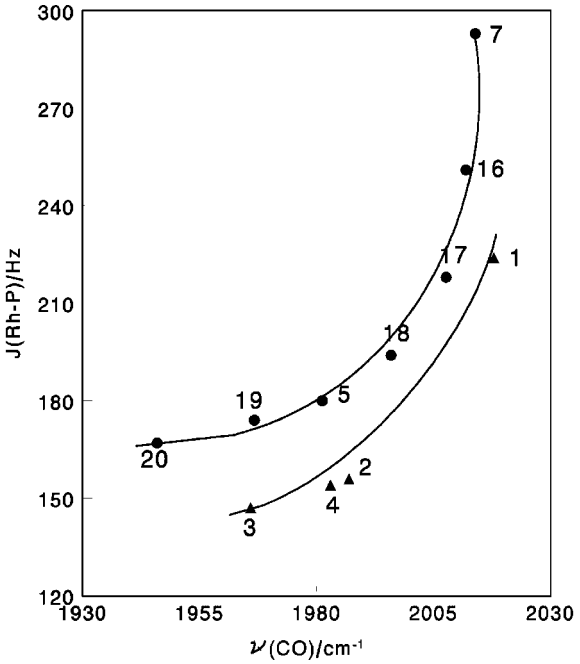

Figure 2. Plot of J(Rh-P) (^{31}P NMR) versus ν(CO) (IR) for RhBp(CO)(P) and Rh(acac)(CO)(P) complexes; RhBp(CO)(P): P = $P(NC_4H_4)_3$ **1**, PPh_3 **2**, PCy_3 **3**, $P(C_6H_4OMe\text{-}4)_3$ **4**; Rh(acac)(CO)(P): P = PPh_3 **5**, $P(OPh)_3$ **7**, $P(NC_4H_4)_3$ **16**, $PPh(NC_4H_4)_2$ **17**, $PPh_2(NC_4H_4)$ **18**, $P(C_6H_4OMe\text{-}4)_3$ **19**, PCy_3 **20**

Table 2. ^{1}H NMR spectroscopic data of bis(pyrazolylborato) ligands in complexes [RhBp(CO)P] (**1**−**4**) measured in $CDCl_3$

Complex	4-H	4′-H	3- or 5-H	3- or 5-H	3′- or 5′-H	3′- or 5′-H
1	5.95	6.27	6.78	7.57	7.63	7.67
2	5.69	6.19	6.29	7.41	7.42	7.56
3	6.06	6.13	7.36	7.46	7.49	7.52
4	5.70	6.18	6.32	6.91	6.94	7.42

(of complexes **1**−**4**) the signals arising from one pyrazolyl ring are better resolved than those in the second ring because of the higher values of the $J_{H,H}$ coupling constants (ca. 2.3 Hz).

The resonances of the 3-H and 5-H protons are observed at δ = 7.3−7.6 ppm, except in the spectra of **2** and **4**, in which one doublet (3-H or 5-H) is present at δ = 6.29 or 6.32 ppm, respectively. In Figure 3 the effect of temperature (in the temperature range from 20 to −60 °C) on the ^{1}H NMR spectra of **2** is presented.

The signals of the 4-H and 4′-H protons (δ = 5.69 and 6.19 ppm) do not change their positions when the temperature is lowered. In contrast, the resonance at δ = 6.29 ppm (3-H or 5-H) is shifted upfield and that at δ = 7.5 ppm (3′-H or 5′-H) is shifted downfield. The dynamics observed can be related only to small changes in the conformation of the pyrazolylborato ligand, because in bis(pyrazolylborato) complexes a change of coordination mode is not expected. The fluxional behaviour of tris(pyrazolylborato) complexes is well documented and is interpreted in terms of a $\kappa^2 \rightarrow \kappa^3$ equilibrium[9,20,21] (N,N-Tp$^-$ or N,N,N-Tp$^-$, respectively).

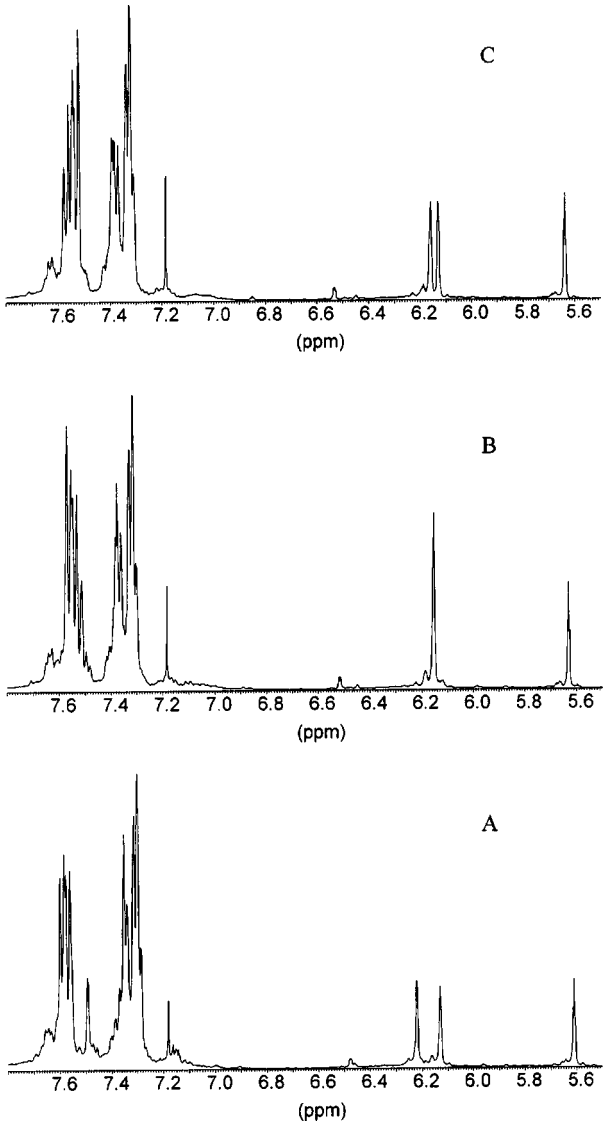

Figure 3. ^{1}H NMR spectra of complex **2** at 20 °C (A), −40 °C (B) and −60 °C (C)

Electrochemical Behaviour of the Rhodium(I) Complexes [RhBp(CO)P]

The cyclic voltammograms of the rhodium(I) complexes [RhBp(CO)P] were run in 0.2 M $[NBu_4][BF_4]/CH_2Cl_2$ (or NCMe), at a Pt- or C-disc electrode. They exhibit, at 200 mV s^{-1} (Table 3), an irreversible oxidation wave (I) at $^{I}E^{ox}_{p/2}$ in the range 0.63−0.95 V vs. NHE, which is followed, at a higher potential ($^{II}E^{ox}_{p/2}$ in the 1.0−1.6 V range), by a second irreversible wave (wave II), with a higher peak-current intensity (Figure 4, for complex **3**). In one case (compound **2**) the shape of the cyclic voltammogram changed rapidly with time, as shown by the alteration of the relative intensities of waves I and II, which is indicative of the instability of the complex in solution.

The oxidation potential of wave I is always substantially lower than that of the free bis(pyrazolylborate) (1.20 V for the KBp salt) and its electrode process is expected[11] to

Table 3. Cyclic voltammetric data for the rhodium(I) complexes [RhBp(CO)P][a]

Complex	P	NCMe		CH_2Cl_2	
		$^{I}E_{p/2}^{ox}$	$^{II}E_{p/2}^{ox}$	$^{I}E_{p/2}^{ox}$	$^{II}E_{p/2}^{ox}$
1	$P(NC_4H_4)_3$	0.95	1.57	1.25	1.69
2	PPh_3	0.80	1.07[b]	0.74	1.27
3	PCy_3	0.63[c]	1.03	0.84[d]	1.20
4	$P(C_6H_4OMe\text{-}4)_3$	0.95[e]	1.44	0.93	1.67
	$[H_2Bp]H$[f]	1.14	–		
	$[H_2Bp]K$[g]	1.20	1.56		

[a] Potentials ($E_{p/2}$ = half-peak potential) in V ± 0.02 vs. NHE measured at a scan rate of 0.2 V s^{-1}, in 0.2 M $[NBu_4][BF_4]$/NCMe or CH_2Cl_2 at a Pt or C electrode. [b] Upon anodic scan, an irreversible cathodic wave is detected at 0.09 V vs. NHE. Relative peak currents of waves I and II change rapidly with time. By CPE (with strong passivation) a total of 4 faraday/mol was obtained (initial step approx. 1.5e). [c] CPE at a potential slightly above that of wave I led to the consumption of only 0.23 faraday/mol, with the disappearance of both waves I and II and the appearance of another wave at E_p^{ox} = 1.57 V. [d] For scan rates higher than 0.6 V/s the wave shows some reversibility. [e] For scan rates higher than 10 V/s the wave shows some reversibility. At 350 V/s it is the only wave detected. [f] Cathodic wave at E_p^{red} = −0.48 V due to H^+ reduction. [g] Cathodic wave at E_p^{red} = −1.53 V which, upon scan reversal, leads to an oxidation wave at 0.26 V.

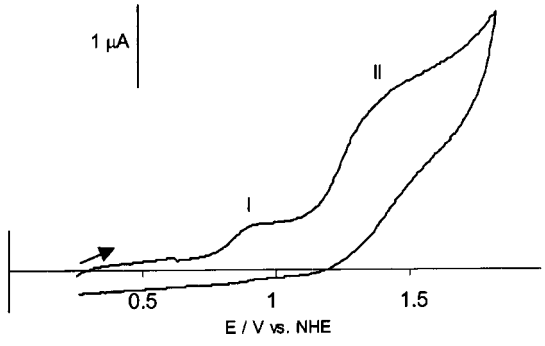

Figure 4. Cyclic voltammogram of complex **3** (2.4 mmol dm^{-3} in CH_2Cl_2 with 0.2 mol dm^{-3} $[NBu_4][BF_4]$) at a carbon disc (d = 0.5 mm) working electrode and at a scan rate of 0.2 V s^{-1}

involve, as the first step, the metal-centered, single-electron $Rh^I \rightarrow Rh^{II}$ oxidation. However, the overall number of electrons involved in each oxidation wave could not be measured due to the strong electrode passivation associated with the electrode processes.

Such an oxidation potential is also much lower (by ca. 0.5−0.7 V) than that exhibited[11] by the corresponding acetylacetonato complexes [Rh(acac)(CO)P], indicating a much stronger electron-donor character of the bis(pyrazolyl)borate ligand than that of acetylacetonate. In fact, the first oxidation potential should reflect the relative electron donor/acceptor abilities of the ligands as measured by the electrochemical E_L ligand parameter proposed by Lever, for which the empirical linear correlation [Equation (1)] has been shown to be applicable to many redox couples.[22,23] The redox potential of the complex (E) is expressed in V vs. NHE, ΣE_L is the sum of the E_L values (V vs. NHE) for all the ligands (additive effects), whereas S_M and I_M (V vs. NHE) depend upon the metal and redox couple, the spin state and the stereochemistry.

$$E = S_M \times (\Sigma E_L) + I_M \quad (1)$$

The E_L value for the bis(pyrazolylborate) ligand (for each of its 2e-donor *N*-coordinating arms) was assumed to be identical to those of the pyrazolate ligand (−0.24 V[22,23]) and of the related hydrotris(pyrazolyl)borate ligand (Tp′; −0.23 V for each of its 2e-donor *N*-coordinating arms) estimated in this study by taking into consideration the oxidation potential data reported[25] for the tetracoordinate Rh^I compounds [Rh(κ²-Tp′)(CO)(P)] [Tp′ = HBR_3 (R = 3,5-dimethylpyrazolyl); P = PPh_3, PCy_3, $P(NMe)_3$, $P(C_6H_4Me\text{-}4)_3$ or $P(C_6H_4Me\text{-}3)_3$] as well as Lever's previously established[11] linear relationship expressed by Equation (1), in which S_M = 1.93 and I_M = −1.29 V.[24] The E_L value thus estimated for Tp′ (−0.23 V for each N-ligating arm) is identical to that of pyrazolate (E_L = −0.24),[22,23] indicating that the pyrazolylborate group has a negligible influence on the σ/π-donor/acceptor properties of the pyrazolate ligand.

This E_L value (−0.24 or −0.23 V for each *N*-coordinating arm) is much lower than that reported for the acetylacetonate ligand (−0.08 V for each *O*-coordinating arm),[22] showing that pyrazolate, and bis- and tris(pyrazolylborate) ligands are much stronger electron-donor ligands than $acac^-$, in agreement with the above-mentioned conclusion based on the much lower oxidation potentials of the Bp^- complexes in this study in comparison with the analogous $acac^-$ complexes.

The order of the measured first oxidation potential values of the complexes (**3** < **2** < **1**, **4**) follows the expected reverse order of the electron-donor ability of the phosphane, i.e. $PCy_3 > PPh_3 > P(C_6H_4OMe\text{-}4)_3$, $P(NC_4H_4)_3$. Since complexes **1** and **4** have an identical oxidation potential, the tris(4-methoxyphenyl)phosphane ligand is pro-

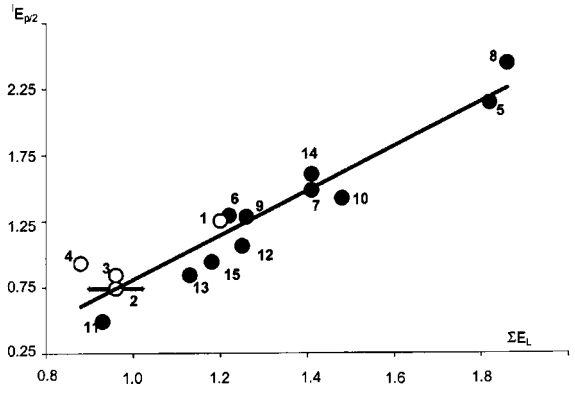

Figure 5. Plot of $^{I}Ep/2^{ox}$ (V versus NHE, measured in CH_2Cl_2) versus ΣE_L (V versus NHE) for [RhBp(CO)(P)] [P = $P(NC_4H_4)_3$ **1**, PPh_3 **2**, PCy_3 **3**, $P(C_6H_4OMe\text{-}4)_3$ **4**] (o) and for other tetracoordinate Rh^I complexes published elsewhere (see text) (•);[11,24] the E_L(L) value of CO taken from the literature (0.99 V) and that of Bp considered (see text) as that of pyrazolate (−0.24 V);[22,23] for $P(C_6H_4OMe\text{-}4)_3$ (complex **4**) the E_L value for tritolylphosphane was considered (0.37 V);[22,23] for PPh_3 an error bar comprising the E_L value taken from the literature (0.39 V)[22,23] and the one estimated from previous data (0.51 V)[11] is presented

posed to exhibit an E_L value identical to that (0.69 V) we have obtained previously[11] for the *N*-pyrrolylphosphane $P(NC_4H_4)_3$.

The rhodium complexes of this study with ligands with known E_L values [**1**, **2** and **3**; for **4** the E_L value of tri(tolyl)-phosphane was taken for $P(C_6H_4OMe\text{-}4)_3$] fit the roughly linear plot of ${}^{I}E^{ox}_{p/2}$ vs. ΣE_L (Figure 5), which also contains the data reported by us[11] for the Rh^I complexes [Rh(O∩O)(CO)L] [O∩O = acac, L = CO **5**, PPh_3 **6**, $P(OPh)_3$ **7**; O∩O = PhC(O)CHC(O)Me (bac), L = CO **8**, PPh_3 **9**; O∩O = PhC(O)CHC(O)CF_3 (bta), L = PPh_3 **10**], as well as those reported by Werner et al. for [RhCl(L)[P*i*Pr_3)$_2$] [L = CPh_2 **11**, C=CPh_2 **12**, C=C=CPh_2 **13**, CO **14** and C_2H_4 **15**].[24]

The novel relationship expressed by Equation (2) (r = 0.95), considering also the complexes in the present study (Figure 6), allows the adjustment of S_M and I_M for the square-planar Rh^I/Rh^{II} redox couples: S_M = 1.68 and I_M = −0.87 V. Values of S_M = 1.93 and I_M = −1.29 V vs. NHE have been proposed previously[24] on the basis of the then available data.

$$E^{ox}_{p/2} = 1.68 \times \Sigma E_L - 0.87 \quad (2)$$

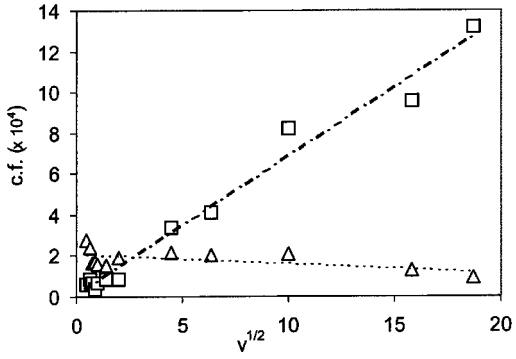

Figure 6. Plot of the current-function $i_p \cdot C^{-1} \cdot v^{-1/2}$ ($A \cdot M^{-1} \cdot V^{-1/2} s^{1/2}$) versus the square root of the scan rate ($V\ s^{-1}$), for waves I (□) and II (Δ) of complex **4** (Scheme 2)

In spite of the above-mentioned strong electrode passivation that normally precluded the controlled-potential electrolysis, in one of the cases (compound **3**) this could be achieved at the anodic wave I, leading to the total disappearance of both oxidation waves of the complex with the consumption of much less than 1 F/mol (ca. 0.2 F/mol). In addition, the reversibility of wave I in compound **4** and its current-function $i_p \cdot C^{-1} \cdot v^{-1/2}$ (i_p = peak current intensity, C = concentration, v = scan rate) increases with the scan rate, with concomitant disappearance of wave II (Figure 6). These observations suggest that wave II may result from the oxidation of a species generated in situ upon oxidation, at wave I, of the starting complex according to an Electron-Transfer-Chain-Catalysis (ETCC)-type process,[34,35] in which $E^0[(Rh')^{ox}/(Rh')^{red}] > E^0[Rh^{ox}/Rh]$, as shown in Scheme 2.

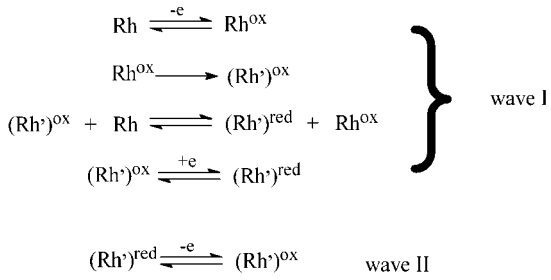

Scheme 2

X-ray Crystal Structures of 2, 3 and [Rh(acac)(CO)PCy_3] (20)

The molecular structures of the complexes [RhBp(CO)PPh_3] (**2**) and [RhBp(CO)PCy_3] (**3**) are shown in Figure 7 and 8, respectively, and selected bond lengths and angles are listed in Tables 4 and 5, respectively. The geometry about the rhodium atoms in both complexes is square planar, as expected for four-coordinate d^8 species, and the two nitrogen atoms of the bis(pyrazolylborato) anion, the carbonyl ligand and the P atom (from phosphane

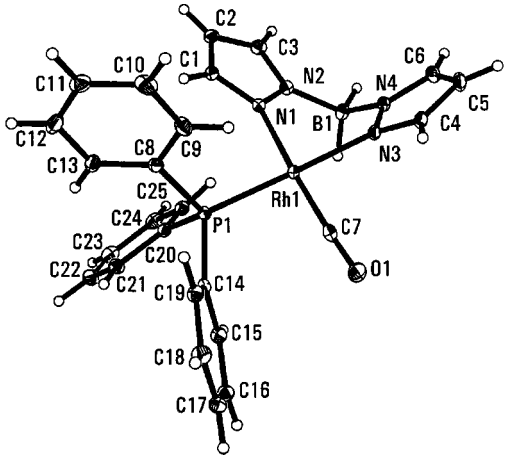

Figure 7. Molecular structure of RhBp(CO)PPh_3 (**2**)

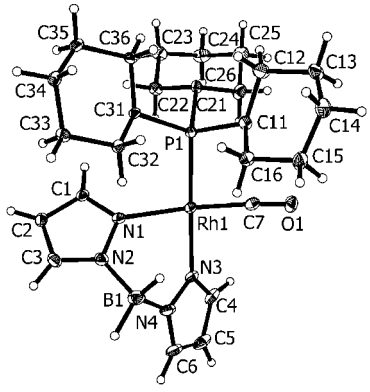

Figure 8. Molecular structure of RhBp(CO)PCy_3 (**3**)

Table 4. Selected bond lengths (Å)

	[RhBp(CO)PPh$_3$] **2**	[RhBp(CO)PCy$_3$] **3**		[Rh(acac)(CO)PPh$_3$][28]	[Rh(acac)(CO)PCy$_3$] **20**		[Rh(N,O)(CO)PPh$_3$] (P *trans* to N)[a]	[Rh(N,O)(CO)PCy$_3$] (P *trans* to N)[b]
Rh−N1	2.0963(16)	2.087(3)	Rh−O1	2.029(5)	2.052(2)	Rh−O	2.040	2.045
Rh−N3	2.0891(15)	2.099(3)	Rh−O2	2.087(4)	2.096(2)	Rh−N	2.054	2.055
Rh−P	2.2614(5)	2.2808(12)	Rh−P	2.244(2)	2.2613(10)	Rh−P	2.279	2.286
Rh−C7	1.815(2)	1.807(5)	Rh−C6	1.801(8)	1.804(4)	Rh−C	1.803	1.788
C7−O	1.144(2)	1.151(5)	C6−O3	1.153(11)	1.160(4)	C−O	1.150	1.156

[a] Average values for complexes [Rh{CF$_3$C(O)CHN(H)Me}(CO)PPh$_3$] and [Rh{CF$_3$C(O)CHN(H)CMe$_3$}(CO)PPh$_3$].[18] [b] Average values for complexes [Rh{CF$_3$C(O)CHN(H)Me}(CO)PCy$_3$] and [Rh{CF$_3$C(O)CHN(H)CMe$_3$}(CO)PCy$_3$].[18]

Table 5. Selected bond angles (°)

Angle	[RhBp(CO)PPh$_3$] (**2**)	[RhBp(CO)PCy$_3$] (**3**)	Angle	[Rh(acac)(CO)PCy$_3$] (**20**)
N1−Rh−N3	87.26(6)	84.83(13)	O1−Rh−O2	87.50(9)
N1−Rh−P	93.05(4)	95.81(10)	O1−Rh−P	88.95(6)
N1−Rh−C7	176.09(7)	174.53(16)	O1−Rh−C6	177.54(12)
N3−Rh−P	176.93(4)	174.99(9)	O2−Rh−P	176.29(7)
N3−Rh−C7	89.54(7)	89.80(16)	O2−Rh−C6	94.60(12)
C7−Rh−P	90.27(6)	89.63(14)	C6−Rh−P	88.93(10)

ligand) are located approximately in the same plane. The Rh−N distances are equal [2.0963(16), 2.0891(15) Å in **2** and 2.087(3), 2.099(3) Å in **3**] within the experimental error (4σ). The Rh−N bonds lengths are similar to those in other complexes with Bp ligands {[RhBp$^{3,5\text{-Me}}{}_2$(C$_2$H$_4$)$_2$] 2.108(5), 2.106(6) Å[26] and [RhBp(PPh$_3$)$_2$] 2.130(2), 2.102(2) Å[26]} and in complexes with κ^2-Tp ligands {[RhTp^{Ph,Me}(CO)PPh$_3$] 2.099(2), 2.120(2) Å[25] and [RhTp^{Me,Me}(CO)PMe$_3$] 2.113(3), 2.101(3) Å[21]}. In β-ketoiminato complexes the Rh−N bonds are significantly shorter (Table 4).

The N1−Rh−N3 angles are slightly different [87.26(6) and 84.83(13)° in **2** and **3**, respectively], which can be explained by the bulkiness of PCy$_3$, represented by a cone angle (Θ) of 170° versus 145° for PPh$_3$.[19]

It is interesting to note that the *trans* effect of the phosphane is not observed, in contrast to [Rh(acac)(CO)PPh$_3$] and **20** (Figure 9) in which the two Rh−O bonds differ by ca. 0.06 Å[27] and 0.04 Å, respectively.

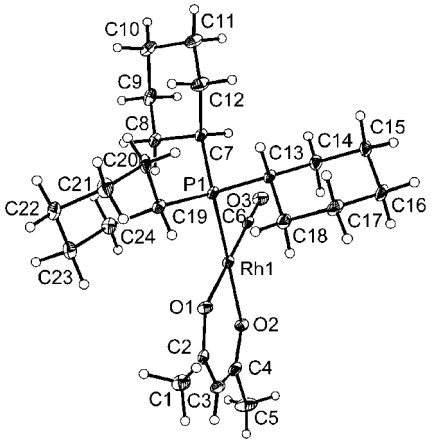

Figure 9. Molecular structure of Rh(acac)(CO)PCy$_3$ (**20**)

The Rh−P bond is longer in complex **3** [2.280(1) Å] than in complex **2** [2.2614(5) Å], as is common for rhodium complexes with PPh$_3$ and PCy$_3$ ligands. The Rh−PPh$_3$ bond in complex **2** [2.2614(5) Å] is longer than those in the related complexes [RhBp(PPh$_3$)$_2$] [2.2261(9) and 2.2503(10) Å][26] and [Rh(acac)(CO)PPh$_3$] [2.244(2) Å],[27] but shorter than that in [RhTp′(CO)PPh$_3$] [2.272(2) Å].[28] The Rh−PCy$_3$ bond in **3** [2.2613(10) Å] is relatively short when compared with the Rh−PCy$_3$ bonds in [RhBp(CO)PCy$_3$] [2.2808(12) Å], [RhTp′(CO)PCy$_3$] [2.292(1) Å],[28] [HRh(CO)(PCy$_3$)$_2$] [2.290(1), 2.297(1) Å][29] and in other acetylacetonatorhodium complexes: [Rh(acac){(*E*)-CH=CHCy}(PCy$_3$)$_2$]BF$_4$ [2.336(3), 2.357(3) Å][30] and [Rh(acac){CH=C=CPh$_2$}(PCy$_3$)$_2$]BF$_4$ [2.285(2) Å].[31] Such a short Rh−PCy$_3$ bond has, until now, only been reported for [Rh(acac)(PCy$_3$)$_2$] [2.252(1), 2.260(1) Å].[30]

A very interesting feature observed in complex **3** is that the angle formed by the rhodium, phosphorus and a carbon atom of one of the cyclohexyl rings [Rh−P−C7 117.53(10)°] differs distinctly from the two remaining angles [Rh−P−C13 110.72(11)° and Rh−P−C19 108.98(12)°]. The same effect has been observed in rhodium complexes with the β-ketoiminate ligand [Rh{CF$_3$C(O)CHC(NH)Me}(CO)PCy$_3$] and [Rh{CF$_3$C(O)CHC(NH)CMe$_3$}(CO)PCy$_3$],[18] and was explained as the result of an interaction between the cyclohexyl ring and the carbonyl ligand. In rhodium-triphenylphosphane complexes, the Rh−P−C(Ph) angles are less differentiated, and in [Rh(acac)(CO)PPh$_3$] they are equivalent.[27] One of the angles between a phosphorus atom and two carbons of one of the cyclohexyl rings in the Rh−PCy$_3$ complexes is also noticeably greater: in **3** the C7−P−C13 and C13−P−C19 angles are ca.104°, whereas the C7−P−C19 angle is ca. 111°. Similar values for the corresponding angles were found for [RhBp(CO)PCy$_3$] and for two complexes with β-

ketoiminate ligands: [Rh{$CF_3C(O)CHC(NH)Me$}(CO)-PCy_3] and [Rh{$CF_3C(O)CHC(NH)CMe_3$}(CO)PCy_3].[18] In analogous complexes with PPh_3 all (Ph)C−P−C(Ph) angles are of similar magnitude.[18]

Catalytic Activity

Complexes **1**−**4** were tested as catalysts in 1-hexene hydroformylation under standardized reaction conditions (80 °C, 10 atm $H_2/CO = 1$) and at different catalyst concentrations and reaction times depending on the catalyst activity observed. The results presented in Table 6 demonstrate the generally high catalytic activity of all complexes, which produce ca. 80% of aldehydes and ca. 20% of 2-hexene when used without any additional free phosphane (the hydroformylation reaction yield increases in the presence of a phosphane co-catalyst[1]). To obtain the best results it is necessary to use a relatively high concentration of catalyst, expressed by a 1-hexene:Rh ratio of 280. However, with complex **3** a 1-hexene:Rh ratio of 800 gave the aldehyde in 78% yield. In reactions with catalysts **1**, **2** and **4** the yield of aldehydes increases with an increase of catalyst concentration. The increase of hydroformylation reaction yield with decrease of the 1-hexene:Rh ratio may be explained as an effect of the competition of the olefin and CO for access to rhodium: at higher concentrations of 1-hexene isomerization is dominant and the main reaction product is 2-hexene. It is interesting to note that the ratio of normal to branched aldehydes (*n*/*iso*) is only slightly dependent on the kind of phosphane coordinated to rhodium — it differs from 1.3 for **3** to 2.8 for **4**. The low *n*/*iso* ratio for **3** could be expected because of the rather strongly basic properties of PCy_3.[19] However, by comparison with results obtained for [Rh(acac)(CO){$P(NC_4H_4)_3$}],[5] one could expect a much higher *n*/*iso* ratio for **1**.

Table 6. Products of 1-hexene hydroformylation catalyzed by complexes **1**−**4**[a]

Catalyst	[1-hexene]/[Rh]	*t* (h)	Aldehydes (%)	2-Hexene (%)	*n*/*iso*
1	800	5	28	70	2.1
	400	3	73	27	2.0
	280	3	86	13	2.3
2	800	5	11	78	2.4
	400	3	37	19	2.6
	280	5	80	20	2.5
3	800	3	78	12	1.3
	280	2	87	11	1.3
4	800	5	44	32	2.8
	400	3	79	21	2.7

[a] Reaction conditions: 80 °C, 10 atm $CO/H_2 = 1$.

The second interesting feature of bis(pyrazolylborato)rhodium catalysts is the relatively high stability of the Rh−N bond under these reaction conditions. This is demonstrated by the presence of [$RhBp(CO)_2$] in all the post-reaction mixtures, as confirmed by the IR spectra, in which two strong ν(CO) bands are observed at 2019 and 2078 cm^{-1}, identical to [$RhBp(CO)_2$] prepared separately.[15] In contrast to [Rh(acac)$(CO)_2$], which reacts easily with CO/H_2 to produce [$Rh_4(CO)_{12}$] and [$Rh_6(CO)_{16}$], [$RhBp(CO)_2$] is not changed when heated at 80 °C under 10 atm CO/H_2 for 5 h. Both dicarbonyl complexes also exhibit different reactivity towards 1-hexene under hydroformylation reaction conditions: [Rh(acac)$(CO)_2$] produces ca. 90% of 2-hexene, and unchanged 1-hexene was found after the reaction with [$RhBp(CO)_2$].

We did not succeed in the isolation of catalytically active forms of rhodium complexes, however at this moment we cannot exclude that rhodium complexes with coordinated pyrazolylborate participate in the catalytic cycle.

Experimental Section

[Rh(acac)$(CO)_2$] was synthesized according to the method described previously.[32] [Rh(acac)(CO)PPh_3] and [Rh(acac)-(CO)PCy_3] (**20**) were obtained from the reaction of [Rh(acac)$(CO)_2$] with an equimolar amount of phosphane in hexane. Crystals of **20** suitable for X-ray analysis were obtained by recrystallization of the complex from toluene/hexane solution. 1-Hexene (Fluka) and toluene were distilled before use.

The electrochemical experiments were performed on an EG & G PAR 273 potentiostat/galvanostat connected to a PC computer through a GPIB interface (National Instruments PC-2A) or on an EG & G PAR 173 potentiostat/galvanostat and an EG & G PARC 175 Universal programmer. Cyclic voltammetry was performed in a two-compartment, three-electrode cell, at a platinum- or carbon-disc working electrode ($d = 0.5$ mm), probed by a Luggin capillary connected to a silver-wire pseudo-reference electrode; a platinum auxiliary electrode was employed. Controlled potential electrolysis was carried out in a two-compartment, three-electrode cell with platinum gauze working and counter electrodes in compartments separated by a glass frit; a Luggin capillary, probing the working electrode, was connected to a silver-wire pseudo-reference electrode. The experiments were performed under an inert atmosphere (N_2) at room temperature, the potentials were measured in 0.2 M $[NBu_4][BF_4]/CH_2Cl_2$ (or NCMe) in the presence of ferrocene as the internal standard, and the redox potential values are quoted relative to the normal hydrogen electrode (NHE) by using the $[Fe(\eta^5\text{-}C_5H_5)_2]^{0/+}$ couple with $E^{ox}_{1/2} = 0.77$ or 0.66 V vs. NHE in 0.2 M $[NBu_4][BF_4]/CH_2Cl_2$ or NCMe, respectively (values obtained relative to NHE by adding +0.24 V[33] to those we measured relative to the SCE). The controlled-potential electrolysis experiments were monitored regularly by cyclic voltammetry, thus assuring that no significant potential drift occurred along the electrolyses. Due to the strong working electrode passivation, the electrolyses had to be interrupted frequently for cleaning of this electrode.

FT-IR spectra were recorded on a Nicolet Impact 400 spectrometer and ^1H NMR spectra on a Bruker 300 MHz, or a Bruker 500 MHz spectrometer. Chemical shifts are referenced to TMS. GC-MS was performed on a Hewlett−Packard 8452A spectrometer.

Synthesis of [RhBp(CO)$P(NC_4H_4)_3$] (1): A mixture of [Rh(acac)$(CO)_2$] (0.11 g, 4.2×10^{-4} mol) and KBp (0.17 g, $9.1 \cdot 10^{-3}$ mol) in benzene (6 mL) was stirred for ca. 1 h. The precipitate of Kacac was separated by filtration, $P(NC_4H_4)_3$ (0.121 g, 5.3×10^{-4}) was added to the filtrate and the solution was stirred for 1 h. The solvent was removed under vacuum and the pale yellow

product was obtained with 89% yield. $C_{19}H_{20}N_7BOPRh$ (507.10): calcd. C 47.94, H 4.20, N 20.16.; found C 47.64, H 4.47, N 19.74. IR (KBr): ν_{CO} 1987 vs; ν_{BH} 2411 m, 2362 m, 2326 w, 2272 w cm^{-1}.

Synthesis of [RhBp(CO)PPh$_3$] (2): KBp (0.06 g, 3.26×10^{-4} mol) was added to a solution of [Rh(acac)(CO)PPh$_3$] (0.107 g, 2.18×10^{-4} mol) in CH_3CN (3 mL). After stirring the mixture for ca. 15 min, the white precipitate of Kacac was removed by filtration. The clear filtrate was evaporated in vacuo giving the orange product in 76% yield. Crystals of **2** were obtained by slow evaporation of the solvents from a toluene/hexane solution. $C_{25}H_{23}N_4BOPRh$ (540.16): calcd. C 55.56, H 4.26, N 10.47; found C 55.71, H 4.30, N 11.00. IR (KBr): ν_{CO} 1987 vs; ν_{BH} 2411 m, 2362 m, 2326 w, 2272 w cm^{-1}. UV/Vis (CH_2Cl_2): λ (ε) = 266 (8500 $M^{-1}\cdot cm^{-1}$), 306 (4100), 360 (2000) nm; (toluene): 308 (4800 $M^{-1}\cdot cm^{-1}$), 360 (2400), 412 (1300) nm.

Synthesis of [RhBp(CO)PCy$_3$] (3): KBp (0.05 g, 2.98×10^{-4} mol) was added to a solution of [Rh(acac)(CO)PCy$_3$] (0.148 g, 2.98×10^{-4} mol) in CH_2Cl_2 (3 mL). After stirring the mixture for ca. 15 min, the white precipitate of Kacac was removed by filtration. The clear filtrate was evaporated in vacuo giving the yellow product in 68% yield. Crystals of **3** were obtained by slow evaporation of the solvents from a benzene/hexane solution. $C_{25}H_{41}N_4BOPRh$ (558.32): calcd. C 53.76, H 7.35, N 10.04; found C 54.09, H 7.53, N 9.69. IR (KBr): ν_{CO} 1966 vs; ν_{BH} 2411 m, 2368 m, 2328 w, 2268 w cm^{-1}. UV/Vis (CH_2Cl_2): λ = 270, 316, 362 nm.

Synthesis of [RhBp(CO){P(C$_6$H$_4$OMe-4)$_3$}] (4): A mixture of [Rh(acac)(CO)$_2$] (0.11 g, 4.2×10^{-4} mol) and KBp (0.17 g, 9.1×10^{-3} mol) in benzene (6 mL) was stirred for ca. 1 h. The precipitate of Kacac was separated by filtration, P(C$_6$H$_4$OMe-4)$_3$ (0.26 g, 7.4×10^{-4} mol) was added to the filtrate and the solution was stirred for 1 h. The solvent was removed under vacuum and the pale yellow product was obtained in 75% yield. $C_{28}H_{29}N_4BO_4PRh$ (630.25): calcd. C 53.38, H 4.60, N 8.89; found C 53.25, H 5.07, N 8.42. IR (KBr): ν_{CO} 1983 vs; ν_{BH} 2421 m, 2418 m cm^{-1}.

Hydroformylation of 1-Hexene: Hydroformylation was carried out at 80 °C in a steel autoclave (50 mL) containing a mixture of 1-hexene and toluene (1.5 mL each). The appropriate amount of catalyst was weighed in a small Teflon vessel and introduced into the autoclave under a nitrogen atmosphere. After introduction of the reagents, the autoclave was closed and filled with an equimolar H_2/CO mixture. The mixture was stirred magnetically and after 2−5 h the autoclave was cooled down. The organic products were separated by vacuum transfer and analysed by GC-MS.

X-ray Studies: Crystal data are given in Table 7, together with refinement details. X-ray data were collected at low temperature using an Oxford Cryosystem device on a Kuma KM4CCD κ-axis diffractometer with graphite-monochromated Mo-K_α radiation (λ = 0.71073 Å). Crystals were positioned at 65 mm from the CCD camera. 612 Frames were measured at 0.75° intervals with a counting time of 20 sec. Accurate cell parameters were determined and refined by a least-squares fit of 1900−2700 of the strongest reflections. The data were corrected for Lorentz and polarization effects. No absorption correction was applied. Data reduction and analysis were carried out with the Oxford Diffraction (Poland) Sp. z o.o (formerly Kuma Diffraction Wrocław, Poland) programs. Structures were solved by direct methods (program SHELXS-97[36]) and refined by the full-matrix least-squares method on all F^2 data using the SHELXL-97[37] programs. Non-hydrogen atoms were refined with anisotropic displacement parameters; hydrogen atoms were included from geometry of molecules and Δρ maps. During refinement they were fixed.

CCDC-215750 (for **20**), -215751 (for **2**) and -215752 (for **3**) contain the supplementary crystallographic data for this paper. These data can be obtained free of charge at www.ccdc.cam.ac.uk/conts/retrieving.html [or from the Cambridge Crystallographic Data Centre, 12 Union Road, Cambridge CB2 1EZ, UK; Fax: (internat.) +44-1223/336-033; E-mail: deposit@ccdc.cam.ac.uk].

Table 7. Crystal data and structure refinement for Rh(acac)(CO)PCy$_3$ (**20**), RhBp(CO)PPh$_3$ (**2**) and RhBp(CO)PCy$_3$ (**3**)

	2	**3**	**20**
Empirical formula	$C_{25}H_{23}BN_4OPRh$	$C_{25}H_{41}BN_4OPRh$	$C_{24}H_{40}O_3PRh$
Molecular mass	540.16	558.32	510.44
T (K)	120(2)	100(2)	100(2)
λ (Å)	0.71073	0.71073	0.71073
Crystal system	monoclinic	monoclinic	monoclinic
Space group	$C2/c$	$C2/c$	$P2_1/n$
a (Å)	20.1610(10)	31.121(6)	10.404(2)
b (Å)	15.2640(10)	8.939(2)	13.091(3)
c (Å)	17.0650(10)	23.893(5)	17.981(4)
β (°)	115.740(10)	127.67(3)	90.00(3)
V (Å^3)	4730.4(5)	5261.2(19)	2449.0(9)
Z	8	8	4
D_c (Mg·m^{-3})	1.517	1.402	1.384
μ (mm^{-1})	0.815	0.734	0.784
F(000)	2192	2312	1072
Crystal size (mm)	0.15 × 0.12 × 0.12	0.15 × 0.15 × 0.07	0.30 × 0.30 × 0.30
θ range for data collection (°)	3.52−28.78	3.43−24.99	3.31−28.71
Ranges of h,k,l	−26→27, −20→20, −15→22	−36→36, −10→8, −28→28	−13→13, −16→17, −21→23
Reflections collected	16508	14851	16678
Independent reflections (R_{int})	5632 (0.0195)	4609 (0.0463)	5763 (0.0651)
Data/parameters	5632/390	4609/298	5763/399
GOF(F^2)	1.138	1.136	1.045
Final R_1/wR_2 indices [$I > 2\sigma(I)$]	0.0276/0.0590	0.0483/0.0864	0.0515/0.0662
Largest diff. peak/hole (e·Å^{-3})	0.605/−0.617	0.934/−0.357	0.810/−0.672

Acknowledgments

This work was supported by the State Committee for Scientific Research KBN (Poland) with the Grant PBZ KBN 15/T09/99/01D. The authors are indebted to Dr. E. Mieczyńska and I. Pryjomska for performing the catalytic tests.

[1] *Applied Homogeneous Catalysis with Organometallic Compounds. A Comprehensive Handbook in Two Volumes* (Eds.: B. Cornils, W. A. Herrmann), VCH, Weinheim, New York, **1996**.
[2] M. P. Magee, W. Luo, W. H. Hersh, *Organometallics* **2002**, *21*, 362.
[3] A. M. Trzeciak, J. J. Ziółkowski, *Coord. Chem. Rev.* **1999**, *190−192*, 883.
[4] A. J. Sandee, J. N. H. Reek, P. C. J. Kamer, P. W. N. M. van Leeuwen, *J. Am. Chem. Soc.* **2001**, *123*, 8468.
[5] A. M. Trzeciak, T. Głowiak, R. Grzybek, J. J. Ziółkowski, *J. Chem. Soc., Dalton Trans.* **1997**, 1831.
[6] A. M. Trzeciak, J. J. Ziółkowski, *Trans. Met. Chem.* **1987**, *12*, 405.
[7] Patent n° P 2058814, **1969**.
[8] D. M. Tellers, S. J. Skoog, R. G. Bergman, T. B. Gunnoe, W. D. Harman, *Organometallics* **2000**, *19*, 2428.
[9] S. Trofimenko, *J. Am. Chem. Soc.* **1967**, *21*, 3120.
[10] S. Serron, J. Huang, S. P. Nolan, *Organometallics* **1998**, *17*, 534.
[11] M. F. C. Guedes da Silva, A. M. Trzeciak, J. J. Ziółkowski, A. J. L. Pombeiro, *J. Organomet. Chem.* **2001**, *620*, 174.
[12] D. E. Graham, G. J. Lamprecht, I. M. Potgieter, A. Roodt, J. G. Leipold, *Trans. Met. Chem.* **1991**, *16*, 193.
[13] A. M. Trzeciak, J. J. Ziółkowski, *Inorg. Chim. Acta* **1995**, *96*, 15.
[14] G. J. J. Steyn, A. Roodt, I. Poletaeva, Yu. S. Varshavsky, *J. Organomet. Chem.* **1997**, *536*, 197.
[15] R. B. King, A. Bond, *J. Organomet. Chem.* **1974**, *73*, 115.
[16] F. Bonati, G. Minghetti, G. Banditelli, *J. Organomet. Chem.* **1975**, *87*, 365.
[17] M. Moszner, S. Wołowiec, A. Trösch, H. Vahrenkamp, *J. Organomet. Chem.* **2000**, *595*, 178.
[18] Yu. S. Varshavsky, M. R. Galding, T. G. Cherkasova, I. S. Podkorytov, A. B. Nikolskii, A. M. Trzeciak, Z. Olejnik, T. Lis, J. J. Ziółkowski, *J. Organomet. Chem.* **2001**, *628*, 195.
[19] C. A. Tolman, *Chem. Rev.* **1977**, *77*, 313.
[20] N. G. Connelly, D. J. H. Emslie, B. Metz, A. G. Orpen, M. J. Quayle, *Chem. Commun.* **1996**, 2289.
[21] K. Chauby, C. Serra Le Berre, Ph. Kalck, J.-C. Daran, G. Commenges, *Inorg. Chem.* **1996**, *35*, 6354.
[22] A. B. P. Lever, *Inorg. Chem.* **1990**, *29*, 1271.
[23] A. B. P. Lever, *Inorg. Chem.* **1991**, *30*, 1980.
[24] I. Kovacik, O. Gevert, H. Werner, M. Schmittel, R. Sollner, *Inorg. Chim. Acta* **1998**, *275−276*, 435.
[25] N. G. Connelly, D. J. H. Emslie, W. E. Geiger, O. D. Hayward, E. B. Linehan, A. G. Orpen, M. J. Quayle, P. H. Rieger, *J. Chem. Soc., Dalton Trans.* **2001**, 670.
[26] M. J. Baena, M. L. Reyes, L. Rey, E. Carmona, M. C. Nicasio, P. J. Perez, E. Gutierrez, A. Monge, *Inorg. Chim. Acta* **1998**, *273*, 244.
[27] J. G. Leipoldt, S. S. Basson, L. D. C. Bok, T. I. A. Gerber, *Inorg. Chim. Acta* **1978**, *26*, L35.
[28] N. G. Connelly, D. J. H. Emslie, W. E. Geiger, O. D. Hayward, E. B. Linehan, A. G. Orpen, M. J. Quayle, P. H. Rieger, *J. Chem. Soc., Dalton Trans.* **2001**, 670.
[29] M. A. Freeman, D. A. Young, *Inorg. Chem.* **1986**, *25*, 1556.
[30] J. G. Leipoldt, G. J. Lamprecht, G. J. van Zyl, *Inorg. Chim. Acta* **1985**, *96*, L31.
[31] M. A. Esteruelas, F. J. Lahoz, M. Martin, E. Onate, L. A. Oro, *Organometallics* **1997**, *16*, 4572.
[32] Yu. S. Varshavsky, T. G. Tcherkasova, *Zh. Neorg. Khim.* **1967**, *12*, 1709.
[33] A. J. Bard, L. R. Faulkner, *Electrochemical Methods*, John Wiley & Sons, New York, **1980**.
[34] M. F. C. Guedes da Silva, C. M. P. Ferreira, J. J. R. Fraústo da Silva, A. J. L. Pombeiro, *J. Chem. Soc., Dalton Trans.* **1998**, 4139.
[35] D. Astruc, *Electron Transfer and Radical Processes in Transition Metal Chemistry*, VCH, Weinheim, 1995, chapter 6.
[36] D. Astruc, *Angew. Chem. Int. Ed. Engl.* **1988**, *27*, 643 and references cited therein.
[37] G. M. Sheldrick, *Acta Crystallogr., Sect. A* **1990**, *46*, 467−473.
[38] G. M. Sheldrick, SHELXL-97, *Program for Crystal Structure Refinement*, University of Göttingen, **1997**.
[39] W. Simanko, K. Mereiter, R. Schmid, K. Kirchner, A. M. Trzeciak, J. J. Ziółkowski, *J. Organomet. Chem.* **2000**, *602*, 59.

Received July 28, 2003
Early View Article
Published Online February 17, 2004

